T$_{1\rho}$ and T$_2$ Quantitative Magnetic Resonance Imaging Analysis of Cartilage Regeneration Following Microfracture and Mosaicplasty Cartilage Resurfacing Procedures

Daniel J Holtzman, BA[1],[†], **Alexander A Theologis, BS**[1],[†], **Julio Carballido-Gamio, PhD**[2], **Sharmila Majumdar, PhD**[2], **Xiaojuan Li, PhD**[2], and **C. Benjamin Ma, MD**[3],[*]

[1]School of Medicine, University of California, San Francisco (UCSF), San Francisco, California, USA.

[2]Musculoskeletal Quantitative Imaging Research (MQIR), Department of Radiology and Biomedical Imaging, UCSF, San Francisco, California, USA.

[3]Department of Orthopaedic Surgery, UCSF, San Francisco, California, USA.

Abstract

Purpose—To examine T$_{1\rho}$ (T1rho) and T$_2$ quantitative magnetic resonance imaging (MRI) in evaluating cartilage regeneration following microfracture (MFx) and mosaicplasty (MOS) cartilage resurfacing procedures.

Materials and Methods—Eighteen patients underwent MFx and eight patients underwent MOS to treat symptomatic focal cartilage defects. Quantitative T$_{1\rho}$ and T$_2$ maps were acquired at 3–6 months and 1 year after surgery. The area of resurfacing was identified, and T$_{1\rho}$ and T$_2$ values for the regenerated tissue (RT) and normal cartilage (NC) were acquired. RT/NC ratios were calculated to standardize absolute T$_{1\rho}$ and T$_2$ values. Data were prospective, cross-sectional, and nonrandomized.

Results—T$_{1\rho}$ and T$_2$ showed good reanalysis reproducibility for RT and NC. Significant differences between RT and NC were present following MFx at 3–6 months for T$_{1\rho}$ and T$_2$ values as well as following MOS at 3–6 months and 1 year for T$_{1\rho}$ values. Following MFx, the T$_2$ RT/NC ratio was significantly different between 3–6 months and 1 year (P = 0.02), while the T$_{1\rho}$ RT/NC ratio approached significance (P = 0.07). Following MOS, the T$_{1\rho}$ and T$_2$ RT/NC ratios were not significantly different between the two timepoints.

Conclusion—T$_{1\rho}$ and T$_2$ MRI are complementary and reproducible methods for quantitatively and noninvasively monitoring regeneration of RT following MFx and MOS.

Keywords

T1rho; T2; MRI; focal cartilage defect; micro-fracture; mosaicplasty

Traumatic knee injuries, often seen in otherwise healthy, active patients, commonly result in focal cartilage defects (CDs) of the weight-bearing articular surfaces of the knee. These

---

[*]Address reprint requests to: C. B. M., Associate Professor, Chief, Sports Medicine and Shoulder Service, University of California, San Francisco School of Medicine, Department of Orthopaedic Surgery, Orthopaedic Institute, 1500 Owens St., San Francisco, CA 94158. maben@orthosurg.ucsf.edu.
[†]Daniel J. Holtzman and Alexander A. Theologis share first authorship for this publication.

defects can be asymptomatic, but swelling, pain, and instability of the joint may occur (1). In addition, chronic degeneration of the cartilage due to altered joint mechanics and loading may predispose the patient to the development of premature osteoarthritis (1). Several surgical options for repair of CDs exist, including microfracture (MFx) and autologous osteochondral mosaicplasty (MOS) surgery. MFx is performed by inducing multiple penetrating injuries into the subchondral bone. Clot formation occurs as well as migration of pluripotent mesenchymal progenitor cells into the area of acute injury, which subsequently differentiate and generate a new articular surface (2). MOS involves transplantation of small cylindrical osteochondral hyaline articular cartilage grafts harvested from the nonweight-bearing surface of the knee into the focal area of cartilage damage (3,4). Autologous chondrocyte implantation and subchondral drilling are other available surgical options but are not the focus of this study. Ideally, any cartilage repair procedure would result in the regeneration of hyaline cartilage that has morphologic and mechanical properties similar to those of native cartilage (5). In practice, fibrocartilage is produced following MFx (6–9), and a mixture of hyaline and fibrocartilage are produced after MOS (3,9,10).

Cartilage biopsy and second-look arthroscopy are currently the gold standards for the evaluation of regenerated tissue (RT) following MFx and MOS (11–13). Second-look arthroscopy allows for direct visualization of the graft surface as well as assessment of the RT's mechanical integrity through indentation measurements (14). Despite these advantages, arthroscopic biopsies are invasive procedures with significant associated surgical morbidity, making routine use impractical and uncommon. In contrast, magnetic resonance imaging (MRI) is a noninvasive method for nonmorbid visualization and evaluation of articular cartilage in the knee (10,14–21). dGEMRIC (delayed gadolinium-enhanced MRI of cartilage), which has been utilized to monitor cartilage repair in humans, requires intravenous or intraarticular injection of gadolinium contrast (14). In this study, $T_{1\rho}$ (T1rho) mapping is utilized in conjunction with T_2 mapping to examine cartilage regeneration following MFx and MOS cartilage resurfacing procedures. These MRI sequences were chosen because they do not require contrast injection and have significant potential for clinical application as additive sequences to traditional qualitative MRI.

Several studies have used T_2 MRI to characterize the biochemical and morphologic properties of normal cartilage (NC) and RT following cartilage repair procedures (10,14–21). Quantitative T_2 mapping has been used specifically for this purpose because it is sensitive to the orientation, concentration, and integrity of collagen, as well as the water content in articular cartilage (22–25). $T_{1\rho}$ imaging describes the spin-lattice relaxation time in the rotating frame and has been proposed as an alternative candidate to measure and assess macromolecular properties and biochemical changes in cartilage content (22,26–30). In addition, $T_{1\rho}$ is sensitive to trypsin-induced proteoglycan loss in bovine cartilage and correlates with proteoglycan content in human cartilage specimens with early degeneration (27,28,31).

While T_2 quantitative MRI has been extensively studied in cartilage repair (10,14–21), no study has examined $T_{1\rho}$ and compared the efficacy of $T_{1\rho}$ and T_2 quantitative MRI in evaluating cartilage regeneration after MFx and MOS cartilage resurfacing procedures. Here we present a nonrandomized prospective cross-sectional study utilizing quantitative $T_{1\rho}$ and T_2 mapping at clinically relevant timepoints in humans following two different and methodologically distinct cartilage resurfacing procedures to assess cartilage regeneration and maturation.

MATERIALS AND METHODS

Subjects

All experiments were approved by the Committee on Human Research at our university and informed consent was obtained from each patient. Eighteen patients (12 men and 6 women; mean age = 36 years) underwent MFx surgery and eight patients (4 men and 4 women; mean age = 36 years) underwent MOS surgery to treat full thickness CDs. All procedures were performed by a single surgeon. The decision of whether to proceed with MFx or MOS was made by the surgeon at the time of surgery. Among other factors, this decision was affected by lesion size, with a larger lesion more likely to be treated by MOS surgery.

Patients were asked to return for follow-up scans within 3–6 months and at 1 year postoperation. These timepoints were chosen because of their clinical relevance. Patients who undergo MFx and MOS are often instructed to maintain nonweight-bearing status for at least 3 months after surgery. Thus, the 3–6 month timepoint would coincide with an initial clinical evaluation before advancement of weight-bearing status and intensification of physical activity. The 1-year timepoint was chosen as it is thought to represent a good clinical endpoint for expected return to previous function and full recovery.

$T_{1\rho}$ and T_2 sequences were obtained at each followup visit. Sixteen patients who underwent MFx were scanned at 3–6 months. Of these 16 patients, four returned at 1 year. Two additional patients who were not scanned at 3–6 months were scanned at 1 year. In total, six MFx patients were scanned at 1 year.

Of the eight total patients who underwent MOS, seven were scanned at 3–6 months. Of these seven patients, six returned at 1 year. One patient who was not scanned at 3–6 months was scanned at 1 year. In total, seven MOS patients were scanned at 1 year. Those patients not scanned at both 3–6 months and 1 year either were unable to make an appointment within the 3–6-month postoperative period or were lost to follow-up following the initial 3–6 month scan. None of these patients were deemed to have failed treatment. In addition, none of these patients underwent reoperation within the study period. Inclusion of patients in this study is summarized in Fig. 1. Data were nonrandomized, gathered prospectively, and analyzed cross-sectionally.

MRI

Patients were scanned using a 3T GE MR scanner (General Electric Healthcare, Milwaukee, WI) using an 8-channel quadrature transmit / 8-channel phased array receive knee coil (General Electric Healthcare, Milwaukee, WI) at 3–6 months (MFx: n = 16; MOS: n = 7) and 1 year (MFx: n = 6; MOS: n = 7) after surgical intervention (n refers to the number of scans). Parallel imaging with array spatial sensitivity technique (ASSET) was performed on all sequences with an acceleration factor of 2. The imaging protocol included sagittal 3D water excitation high-resolution spoiled gradient-echo (HR-SPGR) images and 3D quantitative $T_{1\rho}$ and T_2 mapping. The HR-SPGR images were used to segment each cartilage compartment in the knee, effectively identifying the cartilage of the medial femoral condyle (MFC), lateral femoral condyle (LFC), medial tibial plateau, lateral tibial plateau, trochlea (TROC), and patella. The imaging parameters were: TR/TE = 15/6.7 msec, flip angle = 12°, field of view (FOV) = 14 cm, matrix size = 512 × 512, slice thickness = 1 mm, receiver bandwidth (RBW) = 31.25 kHz, number of excitations = 0.75. The sagittal 3D $T_{1\rho}$-weighted images were acquired using spin-lock techniques and 3D SPGR acquisition as previously developed (32). The duration of the spin-lock pulse was defined as time of spin-lock (TSL), and the strength of the spin-lock pulse was defined as spin-lock frequency (F_{SL}). The number of a pulses after each $T_{1\rho}$ magnetization preparation was defined as views per segment (VPS). There was a relatively long delay (time of recovery, T_{rec}) between

each magnetization preparation to allow enough and equal recovery of the magnetization before each $T_{1\rho}$ preparation. The imaging parameters for the $T_{1\rho}$-weighted images were: TR/TE = 9.3/3.7 msec; FOV = 14 cm, matrix size = 256×192, slice thickness = 3 mm, bandwidth (BW) = 31.25 kHz, VPS = 48, T_{rec} = 1.5 s, TSL = 0, 10, 40, 80 msec, F_{SL} = 500 Hz. Lastly, sagittal 3D quantitative T_2 mapping was acquired by adding a nonselective T_2 preparation imaging sequence (33,34) to the same SPGR sequence as for $T_{1\rho}$ mapping. Imaging parameters of the T_2 sequence were the same as $T_{1\rho}$ except for: TE = 4.1, 14.5, 25, 45.9 msec. All sequences and imaging parameters utilized in this study have been previously validated in phantoms and in vivo (33). The total scan time was ≈20 minutes for $T_{1\rho}$ and T_2 mapping. $T_{1\rho}$ and T_2 mapping were assessed in all subjects.

Cartilage Processing

The images were transferred to and analyzed on a Sun Workstation (Sun Microsystems, Mountain View, CA) for offline data processing. Sites of regenerated tissue (RT) were identified on the HR-SPGR image as regions between cartilage incongruities (Fig. 2). This was performed individually by two observers and was verified by the surgeon who performed the surgeries. The RT region of interest (ROI) corresponded directly with the operative site. The remainder of the articular cartilage surface in the same compartment was identified and was considered NC. Following RT identification, the respective cartilage compartment was semiautomatically segmented on the sagittal HR-SPGR images using in-house software developed with MatLab (MathWorks, Natick, MA) (35). ROIs were subsequently made for RT and NC by dividing the cartilage contours, and the surface area and volume of the lesion was calculated.

An automated iterative minimization process was used to calculate the average thickness for RT and NC. After segmentation, a perpendicular line to the articular cartilage surface and subchondral bone surface was generated automatically in the RT and NC. The cartilage thickness was subsequently determined by calculating the minimum distance from each point on the perpendicular line to a cartilage boundary. The average thickness was calculated for each slice and then averaged for all the slices.

$T_{1\rho}$ and T_2 maps were subsequently reconstructed using a Levenberg–Marquardt monoexponential in-house developed fitting algorithm. $T_{1\rho}$- and T_2-weighted image intensities obtained for different TSLs and TEs were fitted pixel-by-pixel to the following equations, respectively:

$$S(TSL) \propto exp(-TSL/T1\rho)$$

$$S(TE) \propto exp(-TE/T_2)$$

The reconstructed $T_{1\rho}$ and T_2 maps were rigidly registered to the previously acquired high-resolution $T_{1\rho}$- and T_2-weighted SPGR images using the VTK CISG Registration Toolkit (36). The first TSL image and first TE image were used to compute the transformation for $T_{1\rho}$ and T_2 maps, respectively. 3D ROIs for RT and NC were overlaid on the registered $T_{1\rho}$ and T_2 maps. The mean and standard deviation of $T_{1\rho}$ and T_2 values for each ROI were calculated.

Reanalysis Reproducibility Test

The reanalysis reproducibility of the 3D cartilage reconstruction and subsequent measurements of mean $T_{1\rho}$ and T_2 values of RT and NC were evaluated by conducting an

interobserver reliability test. This study included two observers who had each previously segmented more than 25 knee MR images. Each observer separately performed the same segmentation and reconstruction process and identified and calculated $T_{1\rho}$ and T_2 values of RT and NC for all patients. Mean $T_{1\rho}$ and T_2 values were compared. The coefficient of variation (CV, %), defined as 100 times the standard deviation divided by the mean, was calculated for $T_{1\rho}$ and T_2 values of the RT and NC for MFx and MOS procedures.

Data Analysis

For each patient, $T_{1\rho}$ and T_2 values for the RT and NC ROIs were generated. A ratio of RT/ NC was calculated to standardize the absolute $T_{1\rho}$ and T_2 values and allow for averaging among groups of patients and comparison between groups over time. An RT/NC ratio of 1.0 represents equal values for the RT and NC, whereas an RT/NC ratio >1.0 represents increased $T_{1\rho}$ or T_2 signal in the RT relative to the NC, and an RT/NC ratio <1.0 represents increased $T_{1\rho}$ or T_2 signal in the NC relative to the RT. Standard deviations and 95% confidence intervals (CIs) were calculated for each RT/NC ratio to assess for statistically significant differences between RT and NC $T_{1\rho}$ and T_2 average values. A 95% CI that does not overlap with 1.0 is considered statistically significant, as an RT/NC ratio of 1.0 would signify no difference in $T_{1\rho}$ or T_2 values between the RT and surrounding NC.

In addition, $T_{1\rho}$ and T_2 RT/NC ratios at the 3–6-month timepoint were compared to RT/NC ratios at the 1-year timepoint in the same treatment group (MFx and MOS) using an unpaired t-test. A P-value <0.05 is considered statistically significant.

RESULTS

Data were analyzed cross-sectionally. In the group of patients who underwent MFx surgery, average surface area of the focal CDs was 0.54 cm^2. CDs treated by MFx surgery were most commonly found in the MFC (9 out of 18 patients). The LFC ($n = 6/18$), and the TROC ($n = 3/18$) were also sites of CDs in patients who underwent MFx. The defects in the MFC of MFx patients had the largest volume (0.19 cm^3), followed by the LFC (0.14 cm^3) and TROC (0.14 cm^3). In the group of patients who underwent MOS surgery, the average surface area of the CDs was 1.37 cm^2. Among this group, six patients had CDs in the MFC and two patients had defects in the LFC. Defects in the LFC (0.66 cm^3) had a larger volume compared to those in the MFC (0.27 cm^3). On average, CDs treated with MFx had a smaller average surface area and average volume than those treated by MOS (Table 1).

Following MFx surgery, the RT/NC ratio for $T_{1\rho}$ values at 3–6 months was 1.27 [1.13–1.41] (RT/NC ratio [95% confidence interval]) and was 1.06 [0.96–1.16] at 1 year. The RT/NC ratio for T_2 values at 3–6 months was 1.21 [1.10–1.32] and was 0.97 [0.88–1.06] at 1 year (Table 2). Following MOS surgery, the RT/NC ratio for $T_{1\rho}$ values at 3–6 months was 1.07 [1.01–1.13] and was 1.13 [1.02–1.24] at 1 year. The RT/NC ratio for T_2 values at 3–6 months was 1.10 [1.00–1.20] and was 1.03 [0.97–1.09] at 1 year (Table 2). RT/NC ratios for $T_{1\rho}$ and T_2 values calculated for patients 3–6 months and 1 year after MFx and MOS surgery are presented graphically in Fig. 3

Next, we compared the RT/NC ratio for MFx patients at 3–6 months to the ratio at 1 year. The RT/NC ratio for $T_{1\rho}$ values approached a significant difference at 3–6 months and 1 year ($P = 0.07$) and was significantly different for T_2 values at 3–6 months and 1 year ($P = 0.02$) (Fig. 4). Representative $T_{1\rho}$ and T_2 maps are shown at 3–6 months and 1 year with the boundaries of RT and NC demarcated in Fig. 4. The RT at 3–6 months after MFx had an average thickness of 2.3 mm, whereas the NC had an average thickness of 2.2 mm (Fig. 5a). One year after MFx surgery, the RT and NC had average thicknesses of 1.8 mm and 2.1

mm, respectively. Although the thickness of RT decreased over time, the difference was not significant. The thickness of RT was not significantly different from NC at either timepoint.

Following MOS surgery, the RT/NC ratio for $T_{1\rho}$ values was not significantly different between 3–6 months and 1 year, nor was it significantly different for T_2 values at 3–6 months and 1 year (Fig. 6). Representative $T_{1\rho}$ and T_2 maps are shown at 3–6 months and 1 year with the boundaries of RT and NC demarcated in Fig. 6. The RT and NC at 3–6 months after MOS had average thicknesses of 2.2 mm and 2.3 mm, respectively (Fig. 5b). One year after MOS surgery, the RT had an average thickness of 2.1 mm and the NC had an average thickness of 2.3 mm. The thickness of RT was not significantly different from NC at either timepoint, and no significant difference was found between RT thicknesses over time.

The coefficient of variation (CV) interobserver reanalysis reproducibility test of $T_{1\rho}$ and T_2 values showed good reanalysis reproducibility for RT and NC for all patients who underwent either MFx or MOS (CV < 6.0% for all measurements) (Table 3). For RT following MFx, $T_{1\rho}$ had less variability than T_2 (CV = 5.2% and 5.8%, respectively). Conversely, for RT following MOS, T_2 had less variability than $T_{1\rho}$ (CV = 3.7% and 4.3%, respectively). In addition, for NC following both MOS and MFx, $T_{1\rho}$ had less variability than T_2. Overall, $T_{1\rho}$ had lower variability than T_2 (CV = 4.3% and 4.9%, respectively).

DISCUSSION

MFx and MOS represent two common but methodologically different procedures used for the treatment of focal CDs. Of note, MFx and MOS are not the only options for cartilage repair: autologous chondrocyte implantation and other marrow-stimulating procedures are also available. However, MFx and MOS are the most frequently performed cartilage resurfacing procedures and represent two distinct methodologies for cartilage resurfacing of CDs. While technically distinct, MFx and MOS both intend to replace damaged tissue and provide the same mechanical and morphologic support and physiologic function as NC. Ideally, RT from these procedures would provide a stable and supportive joint surface, thus restoring function and preventing the evolution of progressive osteoarthritis in the injured joint.

In reality, the RT generated through MFx and MOS is not identical to the hyaline cartilage seen in NC. MFx generally produces fibrocartilage composed of more collagen and less aggrecan than normal hyaline cartilage (6–9), whereas MOS commonly produces RT that contains a mixture of hyaline cartilage (80%) and fibrocartilage (20%) (3,9,10). While MOS may theoretically result in superior outcomes compared to MFx for the treatment of CDs, both RTs are quite prone to subsequent clinical degeneration, which makes the postoperative and long-term evaluation of the RT's structural and biochemical properties essential in predicting the outcome of cartilage repair procedures and providing patients with appropriate follow-up and counseling (11,13).

Since arthroscopy is quite invasive and unsuitable for longitudinal follow-up, MRI has become the preferred method for noninvasive follow-up of patients after cartilage resurfacing procedures. dGEMRIC imaging, as stated above, requires injection of gadolinium contrast and thus is more invasive and places greater demands on the imaging center and patient. In contrast, $T_{1\rho}$ and T_2 mapping each have the capacity to probe the macromolecular structure of articular cartilage through different mechanisms in a completely noninvasive manner indistinguishable to the patient from traditional qualitative MRI. Ultra-structural alterations to collagen and proteoglycans (PGs) can be detected by changes in $T_{1\rho}$ and T_2 measurements. By using spin-lock techniques, $T_{1\rho}$ is believed to be more sensitive to PG content (27,28,31), while T_2, through its analysis of free water proton

molecule motion within the cartilaginous matrix, is believed to be highly sensitive to the orientation, concentration, and integrity of collagen in articular cartilage (22–25). Despite the distinct features of these two imaging techniques, only T_2 has been used extensively in humans and animals to evaluate the quality of RT following cartilage repair procedures (10,14–21).

Welsch et al (20) examined 20 patients with 3T MRI and diffusion-weighted imaging (DWI) 12 to 63 months after MFx surgery and 12 to 59 months after matrix-associated autologous chondrocyte transplantation (MACT). These scans were correlated with the Lysholm score, a clinical outcomes scoring system of the knee. They found no differences in the Lysholm score between the MFx and MACT groups. However, correlations were found between the Lysholm score and DWI as well as a trend between the Lysholm score and T_2 (20). Similarly, Domayer et al (21) examined 24 patients treated by MFx surgery with 3T MRI and found a moderate correlation between T_2 relaxation times and clinical outcomes, as assessed by the Lysholm score and International Knee Documentation Committee (IKDC) score.

The above studies demonstrate that T_2 imaging is capable of evaluating and detecting differences between normal cartilage and regenerated tissue and correlating these differences with clinical outcomes. However, because CDs are found at varying locations throughout the knee joint, the major limitation to the use of T_2 in assessing CDs is that T_2 measurements are dependent on the cartilage's orientation relative to the main magnetic field (37). It has been shown that the dependence of $T_{1\rho}$ values on the orientation with respect to the main magnetic field is smaller than T_2 values (38), suggesting that $T_{1\rho}$ may be a more precise technique throughout the knee. Thus, in this study we addressed the question: Is $T_{1\rho}$ MRI a more precise method than T_2 for the longitudinal evaluation of the macromolecular framework of RT following MFx and MOS surgery?

The CV reproducibility test measures the reanalysis reproducibility of the semiautomatic segmentation and RT identification. The "overall" reproducibility is also affected by patient positioning, slice localization, and repeatability of the measurement. In our study, the CV for $T_{1\rho}$ and T_2 was less than 6.0% for both MFx and MOS, suggesting good reanalysis reproducibility in evaluating RT and NC following both procedures. Reanalysis reproducibility tests also suggest that $T_{1\rho}$ may be more reproducible for evaluating RT after MOS than for evaluating RT after MFx (CV = 4.3% and 5.2%, respectively). The same trend was observed for T_2 measurements (CV = 3.7% for MOS; CV = 5.8% for MFx). The differences in reproducibility may be a reflection of the fact that fibrocartilage is produced after MFx, and a mixture of hyaline cartilage and fibrocartilage is produced after MOS.

Cartilage thickness data also provide clues to the evolution of RT over time. Although the thickness of RT was not significantly different from NC and was not significantly different over time for both MFx and MOS, a decrease in 0.5 mm in RT thickness after MFx surgery from 3–6 months to 1 year was observed. This decrease, although not significant, may be indicative of postoperative edema that resolves with time or may represent subsequent degeneration that occurs between the two timepoints.

One important limitation of the current study is the number of patients lost to follow-up between the 3–6-month and 1-year timepoints, particularly in the MFx group. In addition, we included patients in the 1-year group who were not imaged at 3–6 months. While we acknowledge that inclusion of all patients, regardless of whether or not they were imaged at both timepoints, limits our ability to make conclusions about changes in RT over time, we feel that it is more important to present our entire patient population than a significantly

smaller group for the first cross-sectional study using $T_{1\rho}$ and T_2 quantitative imaging to prospectively monitor cartilage regeneration following cartilage resurfacing procedures.

When we looked only within each group scanned at a single timepoint instead of between timepoints, we saw differences between RT and NC in MFx patients using $T_{1\rho}$ and T_2 at 3–6 months but not 1 year (Fig. 3). Thus, it is possible that the RT composition significantly changes over time. In fact, Welsch et al (17,19) found that T_2 values of RT declined between their 12–24 month group and their more than 24-month group, which they attributed to a decrease in RT water content and an increase in fibrous tissue, essentially an indication of increased fibrocartilage and deterioration. However, Trattnig et al (39) recently suggested that 1 year of follow up is an acceptable stage at which cartilage maturation can be assessed. The relatively long clinical recovery time following cartilage resurfacing procedures (1 year before return to full activity) is a consequence of the evolving process of cartilage regeneration and maturation following these procedures. While 1 year may be an adequate time period to assess the initial success of cartilage regeneration, continued follow-up is necessary as the long-term success of these procedures will certainly continue to decrease over time as increased cartilage degeneration is likely to occur.

Another limitation of our study is that the full thickness of the RT was studied instead of spatial variations. It is well established that normal articular hyaline cartilage has a predictable zonal variation in $T_{1\rho}$ and T_2 relaxation times, with statistically higher values in the superficial layer relative to the deep layer. While RT lacks the distinct 3D arrangement of collagen of mature cartilage at early stages following repair surgery, as described by Welsch et al (17,19), who showed no variation of T_2 values in deep and superficial layers of MFx regenerated tissue, it is important to assess the spatial variation of more mature RT to determine its similarity to NC. A more detailed analysis of the architecture and macromolecular composition of the RT was performed by White et al (18), in which they acquired the quantitative mean T_2 values of the deep, middle, and superficial layers of the regenerated tissue following MFx and compared them with histologic samples and collagen organization assessed by polarized light microscopy (PLM). They found perfect correlation between organized T_2 and histologic findings of hyaline cartilage and between disorganized T_2 and histologic findings of fibrous reparative tissue (18). Additionally, there was agreement between organized T_2 and normal PLM findings and between disorganized T_2 and abnormal PLM findings (18). Our study did not analyze zonal variation of the RT, and thus, a future goal will be to perform a $T_{1\rho}$ and T_2 laminar analysis of the regenerated tissue following MFx and MOS.

While T_2 has been utilized to monitor cartilage regeneration, these studies have mostly involved autologous chondrocyte transplantation (14–16) and have not extensively examined MFx and MOS, which are extremely common cartilage resurfacing procedures performed on healthy, active patients. $T_{1\rho}$, on the other hand, has not been used to assess cartilage regeneration, but has instead largely been employed to characterize cartilage degeneration associated with osteoarthritis (22). This study represents the first attempt to examine cartilage regeneration using both $T_{1\rho}$ and T_2 quantitative mapping after MFx and MOS cartilage resurfacing procedures in humans. In addition, we chose clinically relevant timepoints of 3–6 months and 1 year to correlate with advancement of weight-bearing status and return to baseline activity, respectively. While neither $T_{1\rho}$ nor T_2 may independently or definitively diagnose success or failure of a cartilage resurfacing intervention with subsequent regeneration or degeneration of cartilage, our hope is that $T_{1\rho}$ and T_2 will provide quantitative evidence that together with clinical markers and the physical examination can be utilized by the clinician to comprehensively evaluate the patient. In addition, because patients who undergo MFx and MOS tend to be young and otherwise healthy, noninvasive monitoring of cartilage resurfacing procedures is absolutely essential.

In conclusion, we have demonstrated that $T_{1\rho}$ and T_2 MRI are complementary and reproducible methods for quantitatively and noninvasively evaluating regenerated tissue following microfracture and autologous osteochondral mosaicplasty cartilage resurfacing procedures for the treatment of symptomatic focal cartilage defects.

Acknowledgments

REFERENCES

1. Messner K, Maletius W. The long-term prognosis for severe damage to weight-bearing cartilage in the knee: a 14-year clinical and radiographic follow-up in 28 young athletes. Acta Orthop Scand 1996;67:165–168. [PubMed: 8623573]

2. Mithoefer K, Williams RJ 3rd, Warren RF, et al. Chondral resurfacing of articular cartilage defects in the knee with the micro-fracture technique. Surgical technique. J Bone Joint Surg 2006;88 Suppl 1(Pt 2):294–304. [PubMed: 16951101]

3. Hangody L, Feczko P, Bartha L, Bodo G, Kish G. Mosaicplasty for the treatment of articular defects of the knee and ankle. Clin Orthop Relat Res 2001:S328–S336. [PubMed: 11603716]

4. Ma HL, Hung SC, Wang ST, Chang MC, Chen TH. Osteochondral autografts transfer for post-traumatic osteochondral defect of the knee-2 to 5 years follow-up. Injury 2004;35:1286–1292. [PubMed: 15561119]

5. Farmer JM, Martin DF, Boles CA, Curl WW. Chondral and osteochondral injuries. Diagnosis and management. Clin Sports Med 2001;20:299–320. [PubMed: 11398360]

6. Furukawa T, Eyre DR, Koide S, Glimcher MJ. Biochemical studies on repair cartilage resurfacing experimental defects in the rabbit knee. J Bone Joint Surg 1980;62:79–89. [PubMed: 7351420]

7. Shapiro F, Koide S, Glimcher MJ. Cell origin and differentiation in the repair of full-thickness defects of articular cartilage. J Bone Joint Surgery 1993;75:532–553.

8. Frisbie DD, Oxford JT, Southwood L, et al. Early events in cartilage repair after subchondral bone microfracture. Clin Orthop Relat Res 2003:215–227. [PubMed: 12567150]

9. Knutsen G, Engebretsen L, Ludvigsen TC, et al. Autologous chondrocyte implantation compared with microfracture in the knee. A randomized trial. J Bone Joint Surg 2004;86-A:455–464. [PubMed: 14996869]

10. Tins BJ, McCall IW, Takahashi T, et al. Autologous chondrocyte implantation in knee joint: MR imaging and histologic features at 1-year follow-up. Radiology 2005;234:501–508. [PubMed: 15616118]

11. Gudas R, Kalesinskas RJ, Kimtys V, et al. A prospective randomized clinical study of mosaic osteochondral autologous transplantation versus microfracture for the treatment of osteochondral defects in the knee joint in young athletes. Arthroscopy 2005;21:1066–1075. [PubMed: 16171631]

12. Bentley G, Biant LC, Carrington RW, et al. A prospective, randomised comparison of autologous chondrocyte implantation versus mosaicplasty for osteochondral defects in the knee. J Bone Joint Surg Br 2003;85:223–230. [PubMed: 12678357]

13. Gudas R, Stankevicius E, Monastyreckiene E, Pranys D, Kalesinskas RJ. Osteochondral autologous transplantation versus micro-fracture for the treatment of articular cartilage defects in the knee joint in athletes. Knee Surg Sports Traumatol Arthrosc 2006;14:834–842. [PubMed: 16552548]

14. Kurkijarvi JE, Mattila L, Ojala RO, et al. Evaluation of cartilage repair in the distal femur after autologous chondrocyte transplantation using T2 relaxation time and dGEMRIC. Osteoarthritis Cartilage 2007;15:372–378. [PubMed: 17110135]

15. Moriya T, Wada Y, Watanabe A, et al. Evaluation of reparative cartilage after autologous chondrocyte implantation for osteochondritis dissecans: histology, biochemistry, and MR imaging. J Orthop Sci 2007;12:265–273. [PubMed: 17530379]

16. Trattnig S, Mamisch TC, Welsch GH, et al. Quantitative T2 mapping of matrix-associated autologous chondrocyte transplantation at 3 Tesla: an in vivo cross-sectional study. Investig Radiol 2007;42:442–448. [PubMed: 17507817]

17. Welsch GH, Mamisch TC, Domayer SE, et al. Cartilage T2 assessment at 3-T MR imaging: in vivo differentiation of normal hyaline cartilage from reparative tissue after two cartilage repair procedures—initial experience. Radiology 2008;247:154–161. [PubMed: 18372466]

18. White LM, Sussman MS, Hurtig M, Probyn L, Tomlinson G, Kandel R. Cartilage T2 assessment: differentiation of normal hyaline cartilage and reparative tissue after arthroscopic cartilage repair in equine subjects. Radiology 2006;241:407–414. [PubMed: 17057068]

19. Welsch GH, Trattnig S, Scheffler K, et al. Magnetization transfer contrast and T2 mapping in the evaluation of cartilage repair tissue with 3T MRI. J Magn Reson Imaging 2008;28:979–986. [PubMed: 18821633]

20. Welsch GH, Trattnig S, Domayer S, Marlovits S, White LM, Mamisch TC. Multimodal approach in the use of clinical scoring, morphological MRI and biochemical T2-mapping and diffusion-weighted imaging in their ability to assess differences between cartilage repair tissue after microfracture therapy and matrix-associated autologous chondrocyte transplantation: a pilot study. Osteoarthritis Cartilage 2009;17:1219–1227. [PubMed: 19409295]

21. Domayer SE, Kutscha-Lissberg F, Welsch G, et al. T2 mapping in the knee after microfracture at 3.0 T: correlation of global T2 values and clinical outcome—preliminary results. Osteoarthritis Cartilage 2008;16:903–908. [PubMed: 18203632]

22. Li X, Benjamin Ma C, Link TM, et al. In vivo T(1rho) and T(2) mapping of articular cartilage in osteoarthritis of the knee using 3 T MRI. Osteoarthritis Cartilage 2007;15:789–797. [PubMed: 17307365]

23. Nieminen MT, Rieppo J, Toyras J, et al. T2 relaxation reveals spatial collagen architecture in articular cartilage: a comparative quantitative MRI and polarized light microscopic study. Magn Reson Med 2001;46:487–493. [PubMed: 11550240]

24. Nieminen MT, Toyras J, Rieppo J, et al. Quantitative MR microscopy of enzymatically degraded articular cartilage. Magn Reson Med 2000;43:676–681. [PubMed: 10800032]

25. Lusse S, Claassen H, Gehrke T, et al. Evaluation of water content by spatially resolved transverse relaxation times of human articular cartilage. Magn Reson Imaging 2000;18:423–430. [PubMed: 10788720]

26. Redfield AG. Nuclear spin thermodynamics in the rotating frame. Science 1969;164:1015–1023. [PubMed: 17796604]

27. Menezes NM, Gray ML, Hartke JR, Burstein D. T2 and T1rho MRI in articular cartilage systems. Magn Reson Med 2004;51:503–509. [PubMed: 15004791]

28. Duvvuri U, Reddy R, Patel SD, Kaufman JH, Kneeland JB, Leigh JS. T1rho-relaxation in articular cartilage: effects of enzymatic degradation. Magn Reson Med 1997;38:863–867. [PubMed: 9402184]

29. Regatte RR, Akella SV, Lonner JH, Kneeland JB, Reddy R. T1rho relaxation mapping in human osteoarthritis (OA) cartilage: comparison of T1rho with T2. J Magn Reson Imaging 2006;23:547–553. [PubMed: 16523468]

30. Akella SV, Regatte RR, Gougoutas AJ, et al. Proteoglycan-induced changes in T1rho-relaxation of articular cartilage at 4T. Magn Reson Med 2001;46:419–423. [PubMed: 11550230]

31. Wheaton AJ, Dodge GR, Elliott DM, Nicoll SB, Reddy R. Quantification of cartilage biomechanical and biochemical properties via T1rho magnetic resonance imaging. Magn Reson Med 2005;54:1087–1093. [PubMed: 16200568]

32. Li X, Han ET, Busse RF, Majumdar S. In vivo T(1rho) mapping in cartilage using 3D magnetization-prepared angle-modulated partitioned k-space spoiled gradient echo snapshots (3D MAPSS). Magn Reson Med 2008;59:298–307. [PubMed: 18228578]

33. Brittain JH, Hu BS, Wright GA, Meyer CH, Macovski A, Nishimura DG. Coronary angiography with magnetization-prepared T2 contrast. Magn Reson Med 1995;33:689–696. [PubMed: 7596274]

34. Foltz WD, Al-Kwifi O, Sussman MS, Stainsby JA, Wright GA. Optimized spiral imaging for measurement of myocardial T2 relaxation. Magn Reson Med 2003;49:1089–1097. [PubMed: 12768587]

35. Carballido-Gamio, J.; Bauer, J.; Lee, KY.; Krause, S.; Majumdar, S. Combined image processing techniques for characterization of MRI cartilage of the knee. 35. Conf Proc IEEE Eng Med Biol Soc; 2005. p. 3043-3046.

36. Rueckert D, Sonoda LI, Hayes C, Hill DL, Leach MO, Hawkes DJ. Nonrigid registration using free-form deformations: application to breast MR images. IEEE Trans Med Imaging 1999;18:712–721. [PubMed: 10534053]

37. Xia Y, Moody JB, Alhadlaq H. Orientational dependence of T2 relaxation in articular cartilage: a microscopic MRI (microMRI) study. Magn Reson Med 2002;48:460–469. [PubMed: 12210910]

38. Akella SV, Regatte RR, Wheaton AJ, Borthakur A, Reddy R. Reduction of residual dipolar interaction in cartilage by spin-lock technique. Magn Reson Med 2004;52:1103–1109. [PubMed: 15508163]

39. Trattnig S, Millington SA, Szomolanyi P, Marlovits S. MR imaging of osteochondral grafts and autologous chondrocyte implantation. Eur Radiol 2007;17:103–118. [PubMed: 16802126]
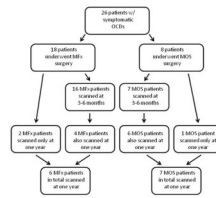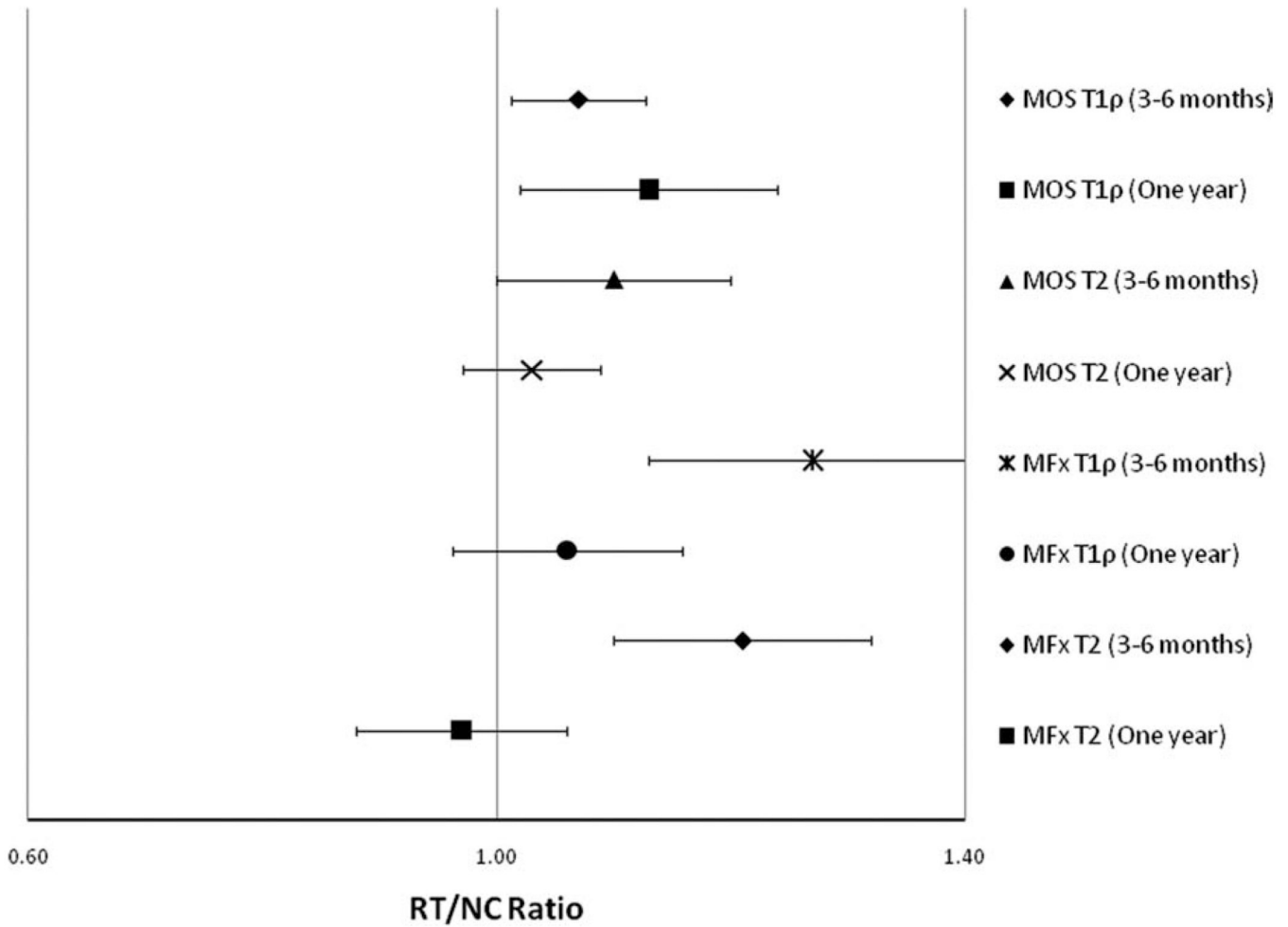
Figure 1.
Flow diagram detailing patients scanned for this study. Sixteen patients who underwent MFx were scanned at 3–6 months. In total, six MFx patients were scanned at 1 year. Seven patients who underwent MOS were scanned at 3–6 months. In total, seven MOS patients were scanned at 1 year. Data is nonrandomized, was gathered prospectively, and was analyzed cross-sectionally. CDs, focal cartilage defects; MFx, microfracture; MOS, mosaicplasty. [Color figure can be viewed in the online issue, which is available at wileyonlinelibrary.com.]
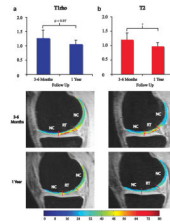
Figure 2.
Representative HR-SPGR image of a patient with a focal CD. Borders of the RT were identified by sites of cartilage incongruity (red arrows) surrounded by NC. [Color figure can be viewed in the online issue, which is available at wileyonlinelibrary.com.]
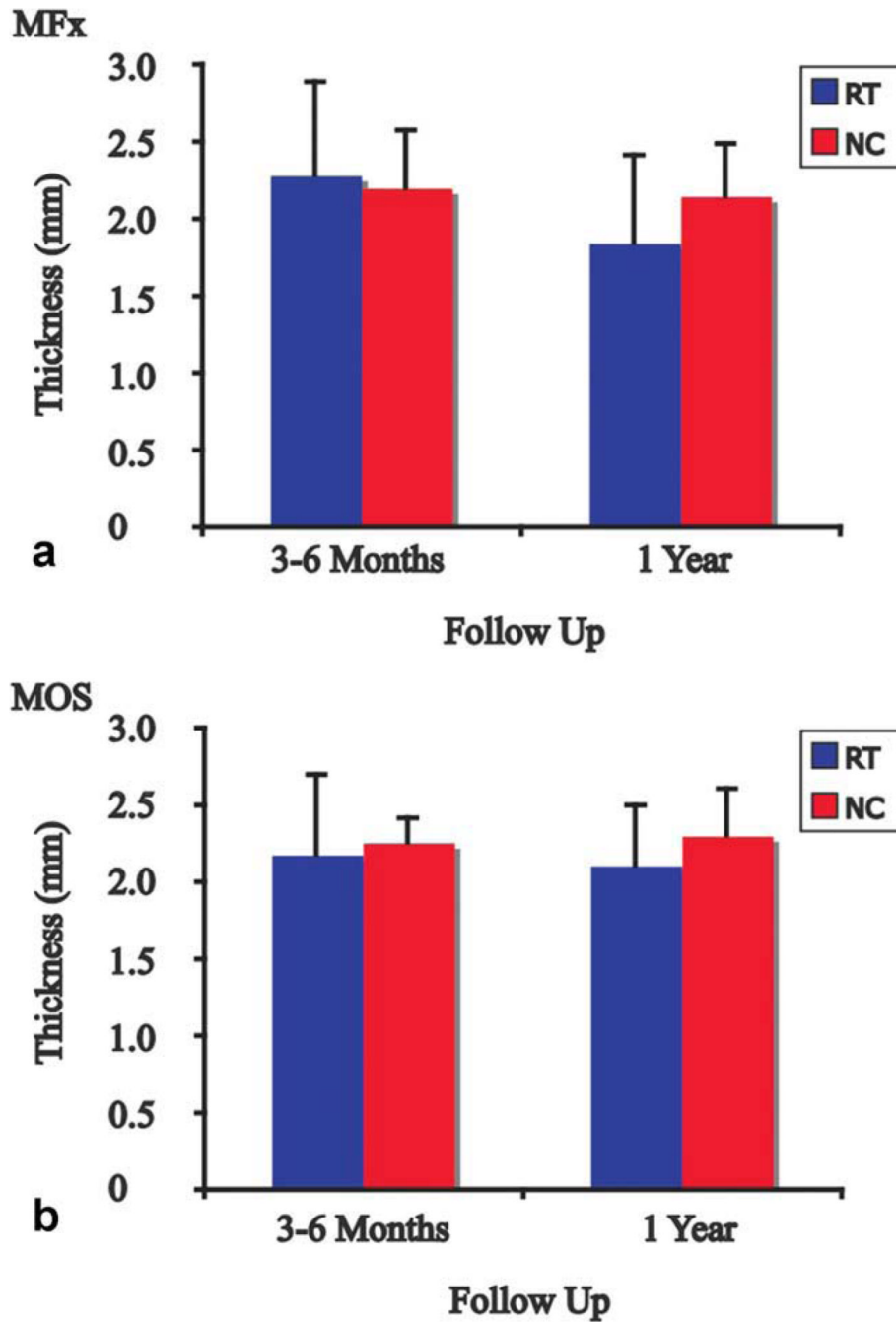
Figure 3.
An RT/NC ratio of 1.0 represents equal values for the RT and NC, whereas an RT/NC ratio >1.0 represents increased $T_{1\rho}$ or T_2 signal in the RT relative to the NC, and an RT/NC ratio <1.0 represents increased $T_{1\rho}$ or T_2 signal in the NC relative to the RT. Errors bars represent the 95% CI for each RT/NC ratio. A 95% CI that does not overlap with 1.0 is considered statistically significant as an RT/NC ratio of 1.0 would signify no difference in $T_{1\rho}$ or T_2 values between the RT and NC. Significant differences between RT and NC are seen in the following groups: MOS $T_{1\rho}$ (3–6 months), MOS $T_{1\rho}$ (1 year), MFx $T_{1\rho}$ (3–6 months), and MFx T_2 (3–6 months). MFx, microfracture; MOS, mosaicplasty; RT, regenerated tissue; NC, normal cartilage. [Color figure can be viewed in the online issue, which is available at wileyonlinelibrary.com.]

Figure 4.
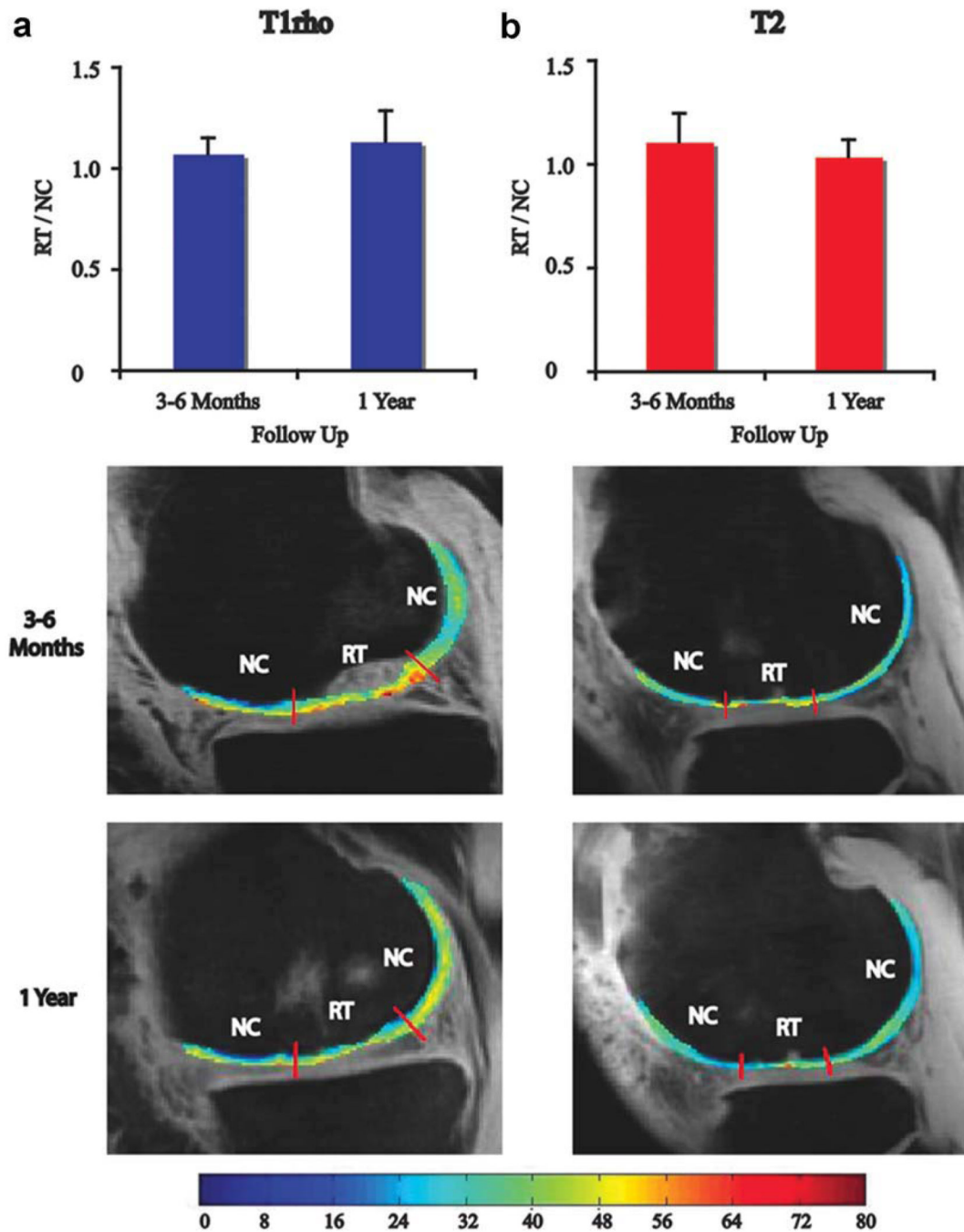(**a**) $T_{1\rho}$ RT/NC ratios and representative $T_{1\rho}$ maps and (**b**) T_2 RT/NC ratios and representative T_2 maps 3–6 months and 1 year after MFx surgery. The RT/NC ratio for $T_{1\rho}$ values was approaching a significant difference between 3–6 months and 1 year (P = 0.07; a) and was significantly different for T_2 values between 3–6 months and 1 year (P = 0.02; b). *Significant difference for T_2 RT/NC ratios between 3–6 months and 1 year; MFx, microfracture; MOS, mosaicplasty; RT, regenerated tissue; NC, normal cartilage.

Figure 5.
Thickness of RT and NC 3–6 months and 1 year after (**a**) MFx and (**b**) MOS surgeries. Thickness of RT was similar to NC at 3–6 months and 1 year after MFx and MOS surgeries, and thickness of NC did not change over time for both procedures. MFx, microfracture; MOS, mosaicplasty; RT, regenerated tissue; NC, normal cartilage. [Color figure can be viewed in the online issue, which is available at wileyonlinelibrary.com.]

Figure 6.
(**a**) $T_{1\rho}$ RT/ NC ratios and representative $T_{1\rho}$ maps and (**b**) T_2 RT/NC ratios and representative T_2 maps 3–6 months and 1 year after MOS surgery. The RT/NC ratio for $T_{1\rho}$ values was not significantly different between 3–6 months and 1 year (a), nor was it significantly different for T_2 values at 3–6 months and 1 year (b). MFx, micro-fracture; MOS, mosaicplasty; RT, regenerated tissue; NC, normal cartilage. [Color figure can be viewed in the online issue, which is available at wileyonlinelibrary.com.]

Table 1

Demographic Information for Patients Who Underwent MFx and MOS Surgery

Treatment	No. patients	Average surface area (cm^2)	Lesion site	No. patients per site	Average lesion volume (cm^3)
MFx	18	0.54	MFC	9	0.19
			LFC	6	0.14
			TROC	3	0.14
MOS	8	1.37	MFC	6	0.27
			LFC	2	0.66

MFx, microfracture; MOS, mosaicplasty; MFC, medial femoral condyle; LFC, lateral femoral condyle; TROC, trochlea.

Table 2

RT/NC Ratios After MFx and MOS Surgery

Treatment/scan	3–6 months (RT/NC [95% CI])	One year (RT/NC [95% CI])
MFx $T_{1\rho}$	1.27 [1.13–1.41]	1.06 [0.96–1.16]
MFx T_2	1.21 [1.10–1.32]	0.97 [0.88–1.06]
MOS $T_{1\rho}$	1.07 [1.01–1.13]	1.13 [1.02–1.24]
MOS T_2	1.10 [1.00–1.20]	1.03 [0.97–1.09]

RT, regenerated tissue; NC, normal cartilage; MFx, microfracture; MOS, mosaicplasty; 95% CI, 95% confidence interval.

Table 3

CV (%) Measuring Interobserver Reanalysis Reproducibility

	$T_{1\rho}$	T_2
RT		
MFx	5.2%	5.8%
MOS	4.3%	3.7%
NC		
MFx	2.7%	4.1%
MOS	2.1%	5.6%
Overall	4.3%	4.9%

CV, coefficient of variation; RT, regenerated tissue; NC, normal cartilage; MFx, microfracture; MOS, mosaicplasty.